Preparation of g-C$_3$N$_4$/Fe$_3$O$_4$/Cu$_2$O composites and their enhanced visible-light photocatalytic performance

Chunhua Cao[1,a], Chunhua Chen[1], Ling Xiao[2]

[1]Key Laboratory of Optoelectronic Chemical Materials and Devices, Ministry of Education, School of Chemical and Environmental Engineering, Jianghan University, Wuhan, P R China

[2]School of Resource and Environmental Science, Hubei Biomass-Resource Chemistry and Environmental Biotechnology Key Laboratory, Wuhan University, Wuhan, P.R. China

[a]cch419@tom.com

Abstract. g-C$_3$N$_4$/Fe$_3$O$_4$/Cu$_2$O composites were prepared successfully by liquid phase reduction-precipitation method with melamine, anhydrous copper sulfate, ferric chloride as the main raw material. The morphology and structure of the composites were characterized by SEM, IR and XRD. Using reactive brilliant red X-3B solution (X-3B) as a model pollutant, the visible-light photocatalytic performance of the composites was compared with pure Cu$_2$O and g-C$_3$N$_4$/Fe$_3$O$_4$. The results showed that Cu$_2$O was inlaided in honeycomb-like g-C$_3$N$_4$ matrix embedded with Fe$_3$O$_4$ nanoparticles, and g-C$_3$N$_4$/Fe$_3$O$_4$/Cu$_2$O composites had good magnetically separable performance. Compared with pure Cu$_2$O and g-C$_3$N$_4$/Fe$_3$O$_4$, g-C$_3$N$_4$/Fe$_3$O$_4$/Cu$_2$O composites exhibited enhanced efficiency for photocatalytic degradation of X-3B under visible light irradiation.

Introduction

The semiconductor composites have been regarded as promising materials applied in dealing with energy shortages and environmental pollution [1,2]. As an old p-type semiconductor, cuprous oxide (Cu$_2$O) has received much attention due to its narrow band gap, low toxicity and low production cost [3,4]. However, the photocatalytic activity of pure Cu$_2$O is relatively low because of the easy recombination between photo-generated electrons and holes. In recent years, a novel metal-free polymeric material, graphitic carbon nitride (g-C$_3$N$_4$) as a n-type semiconductor photocatalyst was reported extensively owing to its chemical stability and narrow band gap energy of 2.7eV [5,6]. The p-n heterojunction structure in the semiconductor composites can improving separation efficiency of photogenerated charge carriers and enhancing the photocatalytic activity and stability of composites [4]. In addition, magnetically separable photocatalysts could be easily separated and collected with magnetic field, which is important from the perspective of reusability, it is also important to avoid the adverse biological effects of the semiconductor nanoparticles [7,8]. Herein, we prepared g-C$_3$N$_4$/Fe$_3$O$_4$/Cu$_2$O composites through reduction-precipitation method.The microstructure characteristics were determined. The visible-light photocatalytic performance of the prepared composites was studied through the photocatalytic decolorization of reactive brilliant red X-3B (X-3B) dye.

Experimental

Materials. The dye, reactive brilliant red X-3B (X-3B) was purchased from ShunKe Chemical Dyestuff Co., Ltd. (Shanghai, China). Other chemical reagents were analytical grade and used without further purification.

Preparation of photocatalysts. g-C$_3$N$_4$ was synthesized by thermal polycondensation of melamine[9], and then treated in concentrated sulfuric acid. g-C$_3$N$_4$/Fe$_3$O$_4$ composites (the mass ratio of g-C$_3$N$_4$ and Fe$_3$O$_4$ is 3:2) were in situ prepared by the reduction-precipitation method described in our previous report [8]. The g-C$_3$N$_4$/Fe$_3$O$_4$/Cu$_2$O composites (g-C$_3$N$_4$/Fe$_3$O$_4$/Cu$_2$O) were synthesized via one-step process as follows: 1.68 g as-prepared g-C$_3$N$_4$/Fe$_3$O$_4$ were dispersed in 50 ml 0.2 mol/L CuSO$_4$·5H$_2$O

solution. The obtained mixture was then kept in water bath at 54 ℃ with magnetic stirring and pH value was adjusted to about 10 using 40 mL 1 mol/L sodium hydroxide solution. The blue precipitate suspension appeared soon. Then reducer glucose (0.01 mol) were added into above suspension solution under continuous stirring, and the color gradually changed into reddish brown. Finally, the reddish-brown products were collected with the aid of an adscititious magnet and washed with distilled water and absolute ethanol for several times, respectively, then dried in vacuum oven at 60 ℃. For comparison, pure Cu_2O powders were also prepared using the same conditions and method mentioned above.

Analysis instruments. The SEM images were taken with a SU8010 high resolution field emission scanning electron microscopy (Hitachi, Japan).The XRD patterns of the samples were recorded by an X'Pert Pro X-ray diffractometer (PANalytical, Holland) with Cu Kα radiation (λ = 1.5406 Å) at a scanning rate of 0.026°/s from 10° to 80° (2θ). The FT-IR spectra were obtained on a Tensor 27 infrared spectrometer (Bruker, German) with a KBr pellet in the range of 4000-400 cm⁻¹.

Photocatalytic decolorization experiments. The photocatalytic performance of samples was evaluated using X-3B degradation in aqueous solution under visible-light irradiation. Experiments were carried out in a quartz reactor. Typically, 60 mg of as-prepared photocatalyst was dispersed in 100 mL of 10 mg/L dye X-3B solution (pH=5.6) with gently stirring for 30 min to ensure adsorption/desorption equilibrium, and then the suspension was exposed to a 500 W tungsten-halogen lamp (λ_d=584 nm) which was located at a distance of 150 mm above the surface of the solution. At given irradiation time intervals, about 4mL supernatant was extracted and separated by an external magnetic field, and the absorbance of the supernatant was measured by TU-1810 UV-vis spectrophotometer at 538 nm in order to determine the concentration of X-3B.

The photocatalytic decolorization rate (D/%) was calculated by the following Eq. (1):

$$D(\%) = \frac{c_0 - c_t}{c_0} \times 100 \tag{1}$$

Where c_0 is initial X-3B concentration (mg/L), c_t is the X-3B concentration at time t minutes (mg/L).

Results and Discussion

XRD analysis. Fig. 1 shows the XRD patterns of g-C_3N_4, g-C_3N_4/Fe_3O_4 and g-C_3N_4/Fe_3O_4/Cu_2O. It can be seen in curve a that there was a distinct peak $2\theta = 27.8°$ corresponding to interlayer stacking of

aromatic
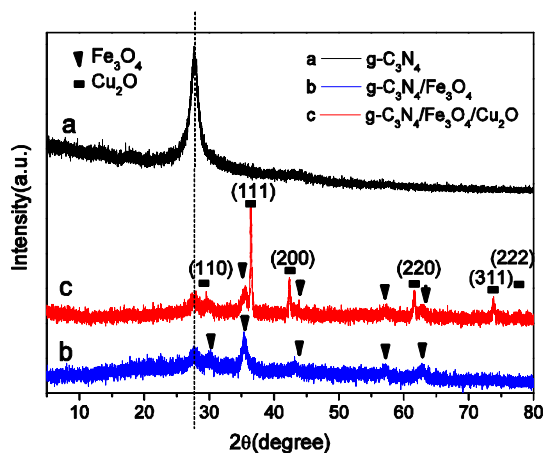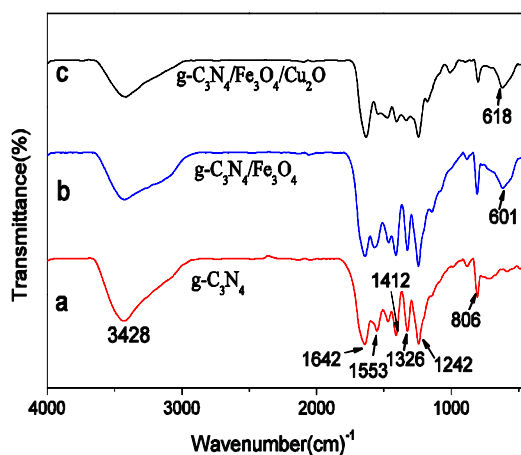
Fig. 1 XRD patterns of samples   Fig. 2 FTIR spectra of samples

segments of (002) plane for graphitic materials. After coupling g-C_3N_4 with Fe_3O_4, the peak decreased and meanwhile, five clear diffraction peaks assigned to a face-centered cubic Fe_3O_4 structure were observed in curve b, indicating the successful sedimentation of Fe_3O_4 onto the surface of g-C_3N_4 and

the well-crystallization of Fe_3O_4 particles. In the XRD pattern of g-C_3N_4/Fe_3O_4/Cu_2O (curve c), besides typical peaks of g-C_3N_4 and Fe_3O_4, there were six clear peaks corresponding to the crystal planes of (110), (111), (200), (220), (311) and (222) of cubic-structured Cu_2O, respectively. These results revealed that Cu_2O particles were in situ formed in g-C_3N_4/Fe_3O_4/Cu_2O and the crystal structures of Fe_3O_4 and Cu_2O were kept unchanged in the composites.

FTIR analysis. The FTIR spectra of g-C_3N_4, g-C_3N_4/Fe_3O_4 and g-C_3N_4/Fe_3O_4/Cu_2O were applied as shown in Fig. 2. Three characteristic absorption regions of g-C_3N_4 at 3428cm^{-1}, 1242~1642cm^{-1} and 806cm^{-1} are observed in Fig. 2a. Similarly, these absorption regions were also observed in the spectrogram of g-C_3N_4/Fe_3O_4 (curve b) and g-C_3N_4/Fe_3O_4/Cu_2O (curve c). Meanwhile, the characteristic adsorption peak at 601 cm^{-1} corresponding to the Fe-O bond vibration of Fe_3O_4 appeared in the spectrum of g-C_3N_4/Fe_3O_4 (curve b), and the characteristic adsorption peak at 618 cm^{-1} corresponding to the Cu-O bond vibration of Cu_2O appeared in the spectrum of g-C_3N_4/Fe_3O_4/Cu_2O (curve c). These results showed the successful formation of g-C_3N_4/Fe_3O_4 and g-C_3N_4/Fe_3O_4/Cu_2O composites.

Morphological analysis. The morphology and surface of g-C_3N_4, g-C_3N_4/Fe_3O_4 and g-C_3N_4/Fe_3O_4/Cu_2O was studied by SEM, as shown in Fig. 3. It could be seen from Fig. 3a that g-C_3N_4 presented honeycomb-like shape and smooth surface. In contrast, g-C_3N_4 in Fig. 3b had rough surface because Fe_3O_4 nanoparticles were formed successfully on the surface of honeycomb-like g-C_3N_4. From Fig. 3c, we could find that Cu_2O was inlaided in g-C_3N_4 matrix embedded with Fe_3O_4 nanoparticles, further indicating the successful formation g-C_3N_4/Fe_3O_4/Cu_2O composites.
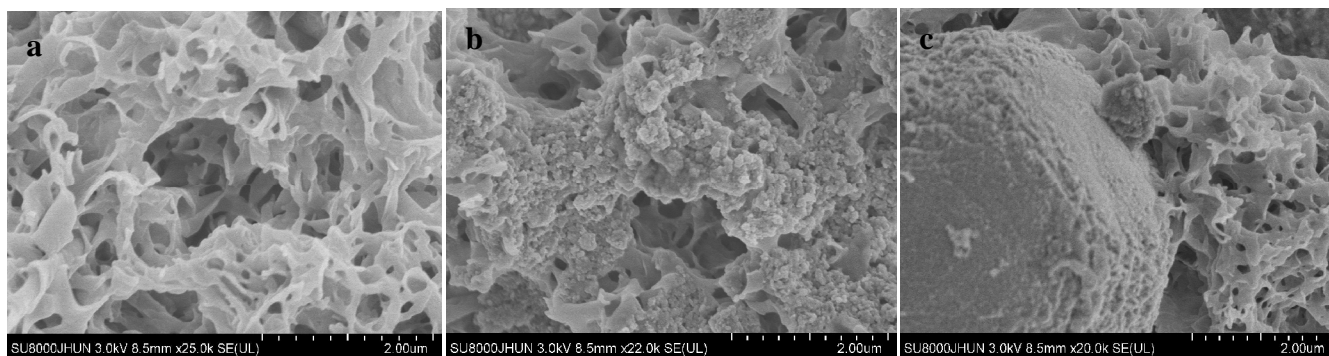
Fig.3 SEM images of g-C_3N_4 (a), g-C_3N_4/Fe_3O_4 (b) and g-C_3N_4/Fe_3O_4/Cu_2O (c)

Magnetic and photocatalytic performance. The magnetic and enhanced visible-light photocatalytic performance of g-C_3N_4/Fe_3O_4/Cu_2O were illustrated in Fig.4. As seen in Fig. 4, after 60 min
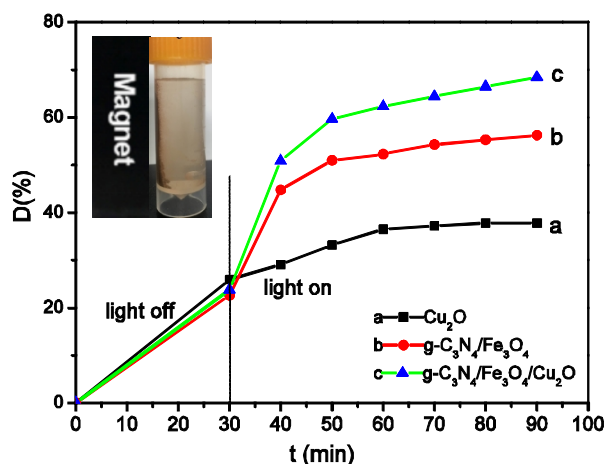
visible-light

Fig.4 The photocatalytic decolorization curves of X-3B dye using g-C_3N_4 (a), g-C_3N_4/Fe_3O_4 (b) and g-C_3N_4/Fe_3O_4/Cu_2O (c) as catalyst under visible light irradiation. Inset shows the photographs of g-C_3N_4/Fe_3O_4/Cu_2O attracted to the place near the magnet outside the vessel.

irradiation, under constant dye initial concentration (10mg/L) and catalyst amount (0.6g/L), the photocatalytic degradation rate of X-3B over the g-C_3N_4/Fe_3O_4/Cu_2O composites could reach about 70%, much higher than that over pure Cu_2O and g-C_3N_4/Fe_3O_4. Moreover, inset in Fig. 4 shows the photograph of g-C_3N_4/Fe_3O_4/Cu_2O attracted to the place near the magnet in aqueous solution by applying a magnet outside the vessel. The results above suggested that g-C_3N_4/Fe_3O_4/Cu_2O composites presented good magnetically separable and enhanced visible-light photocatalytic performance.

Conclusions

Novel g-C_3N_4/Fe_3O_4/Cu_2O composites were constructed via a facile and low-temperature liquid phase reduction-precipitation process. The g-C_3N_4/Fe_3O_4/Cu_2O composites had enhanced visible-light photocatalytic activity as well as good magnetically separable performance through combining the advantages of p-type Cu_2O photocatalysts, n-type semiconductor g-C_3N_4 and Fe_3O_4 magnetic particles.

Acknowledgements

References

[1] Y. L. Tian, B. B. Chang, J. Fu, B.C. Zhou, J. Y. Liu, F. N. Xi, X. P. Dong: J. Solid State Chem. Vol. 212 (2014), p. 1.

[2] R. Shi, J.Lin, Y. J. Wang, J. Xu, Y. F. Zhu: J.Phys.Chem.C Vol. 114 (2010), p. 6472.

[3] M.A. Shoeib, O.E. Abdelsalam, M.G. Khafagi, R.E. Hammamd: Adv. Powder Technol. Vol. 23 (2012) p. 298.

[4] C. H. Cao, L. Xiao, C. H. Chen, Q. H. Cao: Appl. Surf. Sci. Vol. 357 (2015) p. 1171.

[5] X.Wang, K. Maeda, A. Thomas, K. Takanabe, G. Xin, J. M. Carlsson, K. Domen, M. Antonietti: Nat.Mater. Vol. 8 (2009), p.76.

[6] X. Wang, Q. Wang, F. Li, W. Yang, Y. Zhao, Y. Hao, S. Liu: Chem.Eng.J. Vol. 234 (2013), p. 361.

[7] R. Chalasani, S. Vasudevan: ACS nano Vol. 7 (2013), p. 4093.

[8] C. H. Cao, L. Xiao, C. H. Chen, Q. H. Cao: Appl. Surf. Sci. Vol. 333 (2015) p. 110.

[9] Y. Zheng, J. Liu, J. Liang, M. Jaroniec, S. Z. Qiao: Energy Environ. Sci. Vol. 5 (2012), p. 6717.